# High-Resolution Aerial Radiation Mapping for Nuclear Decontamination and Decommissioning - 17371

Peter G. Martin *, Thomas B. Scott *, Oliver D. Payton *, and John S. Fardoulis *
* University of Bristol, United Kingdom, BS8 1TH

## ABSTRACT

Unmanned aerial vehicles (UAVs) are now widely employed as part of numerous applications including defence, search and rescue as well as within scientific fields such as high-altitude atmospheric sampling and remote sensing, to name but a few. However, their application to the high-resolution detection of radiation anomalies (specifically as part of the routine monitoring on nuclear sites) has been less well explored. In this work, we present the results of the radiation monitoring via a lightweight aerial platform on an active nuclear site (Sellafield Ltd.); having already deployed the device in the Fukushima-contaminated region. The system employed was able to detect regions of elevated radiation at the sub-meter scale as well as attributing the species responsible. Such a system presents an extremely powerful tool where it is not desirable, nor practical, to send human operators. Results presented show that the platform is easily capable of operating within the challenging and confined settings of a site such as Sellafield (or other similar sites worldwide).

## INTRODUCTION

The decommissioning of the worlds legacy nuclear sites presents a significant technical challenge as well as large financial cost. In the UK, the Sellafield Ltd. nuclear licensed site, located on the Cumbrian coast, is the location at which all of the UK's (as well as several other countries) legacy wastes are currently being reprocessed for use within further power generation or final storage and disposal. As part of the long-term plan for the 3 km² site, it is targeted that all operations on-site will have been completed in a little over 100 years, by the year 2120, with the process of post-operational clean-out (POCO) of a number of former facilities well underway around the site [1]. The estimated costs of this withdrawal, including full decommissioning and withdrawal is estimated to cost in-excess of £80 billion ($100 billion). By the end of all remedial works at the site, it is targeted that no residual radiological contamination will exist [1].

Unlike other larger sites that exist for the reprocessing of spent nuclear material around the world; at only 3 km™, the Sellafield site is only 1/500$^{th}$ of the area of the US DoE Hanford Site [2] – and as a result presents a range of unique challenges due to the varied amount of infrastructure that is found in such a confined area. On the site there are a total of 7 decommissioned reactors, the centralised storage facility for the countries high-level nuclear wastes (in the current absence of a suitable long-term geological disposal facility), considerable reprocessing operations, legacy material stores as well as hundreds of additional buildings involved in active material handling [1]. The site also comprises a large number of administrative and clerical

buildings associated with the on-site operations. As the first activity on the site began associated with the commencement of the UK's nuclear weapons program (construction of the Windscale Piles) to generate weapons grade material and the facilities to power it – little consideration was given to future practicalities of eventual site closure and routine monitoring of radiation on the site.

This routine monitoring of radiation in order to assess both the existence and any time-resolved migration is nearly always performed by humans equipped with handheld survey instruments. As well as the obvious issues surrounding access to complicated buildings and structures during such works (physically and administratively), additional negatives arise from the radiation exposure sustained from working in close proximity to potentially highly-contaminated areas and the slow rate at which an area can be covered on foot. In contrast, the use of high-altitude (manned) surveys; typically employed for regional-scale geophysical and radiological measurements [3,4], are not appropriate for the high-resolution monitoring for decontamination and decommissioning as a result of the inherently high altitudes (150 to 700 m) [5] at which they operate and hence the low on-ground spatial resolution they attain.

The application of high-resolution aerial radiation mapping, as an existing technology, is a powerful tool for routine site monitoring, decontamination and decommissioning with numerous advantages over other methods. Future developments in low-altitude systems, such as for automated emergency monitoring (utilising advancements in swarm behaviour and artificial intelligence) and release sampling, are exciting potential applications of this technology in the not too distant future.

## METHOD

### Unmanned Aerial Vehicle (UAV)

There currently exists an extensive range of unmanned aerial vehicles, more informally termed "drones" – ranging from tiny handheld craft to extremely large systems of a size not dis-similar in dimension to manned aircraft. Each platform design has its own specific advantages (and disadvantages), being employed for their unique application(s).

The work described herein uses an X8 configuration UAV designed and constructed at the University of Bristol, with full details of the platform and full design parameters available in published works by the authors [6,7]. The selection of the X8 configuration (with pairs of propellers mounted both above and below the platforms four arms) was made to ensure system redundancy in the event of motor / propeller failure mid-flight. Controlled via either or a combination of both manual radio controls and pre-programmed GPS waypoints, the UAV was capable of flight of up to 30 mins duration (on LiPo batteries), at altitudes of 5 – 50 m and velocities of up to 50 km/h. The total weight of the UAV was 7.0 kg, a mass determined not to represent a danger to structures on the Sellafield site should an impact ever occur. Selection of carbon-

fibre propellers over plastic types for the UAV ensured that if a collision should occur with birds during a flight, then they would shatter instantly rather than remaining partially in-tact and subsequently impacting on flight performance / stability.

The construction of the UAV, with a large area located directly below the flight batteries / control system, between the platforms legs (Fig. 1) allows for the attachment of differing sensor payloads or imaging devices. For the high-resolution detection and mapping of radiation anomalies, a 500 g payload consisting of a miniaturised gamma-spectrometer and rangefinder was used.

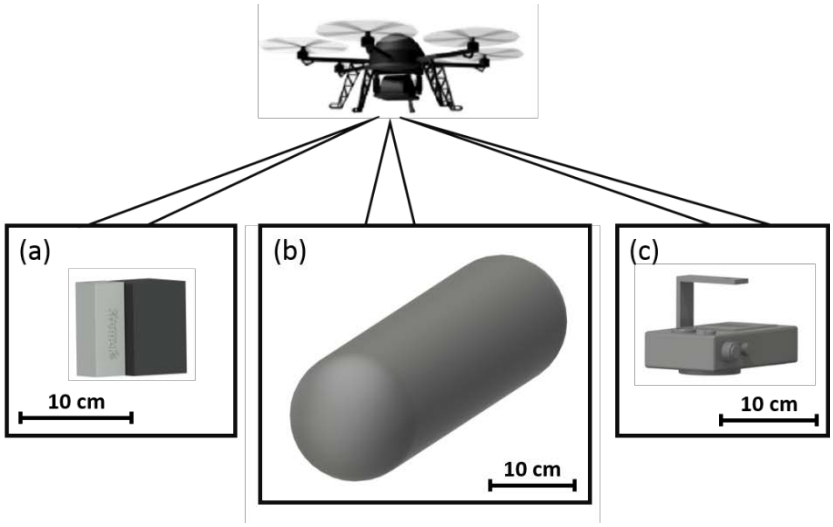


**Fig. 1.** Unmanned aerial vehicle (UAV) with the available attachable detection options; (a) gimballed micro gamma-spectrometer, (b) 3D-scanning LiDAR-pod (Routescene Ltd.) and (c) conventional digital imaging cameras.

## Detection Payload

As mentioned above, the detection system employed for this work was extremely lightweight in comparison to systems capable of being carried by larger aerial platforms – weighing only 500 g – carried under the airframe (Fig. 1a), described in earlier works by the authors [6,7]. Using specially-written software, both a gamma-ray spectrometer (Kromek GR1™, Co. Durham, UK) and a single point laser rangefinder were used, mounted side-by-side on an active gyro-stabilised gimbal (to ensure both remained normal to the ground surface during UAV flight). The gamma-ray spectrometer recorded the incident gamma-photons as a string of calibrated energy bins – with the total number of readings representing the number of counts per second (CPS) recorded by the detector. Each of these strings of values was combined with a value for its location (and altitude) obtained by an on-board GPS unit as well as a value for the height of the system above the ground from the single-point rangefinder (AR2500™, Acuity®) [8], with an accuracy of ±5 cm over a 250 m range. Sampling was taken at an interval of every 0.5 seconds (2 Hz), with the values integrated to give results as CPS.

Through the subtraction of the rangefinder-derived data from the GPS altitude, a crude elevation model of the area can be constructed, onto this the radiation intensity data can be applied for simplistic visualisation. Due to the inherent flexibility of the mounting options that the UAV presents, a high-resolution 3-dimensional scanning LiDAR unit is capable of being transported under the aerial system (Fig. 1b). Unlike the single-point system, this device uses a total of 32 individual lasers, rastering as a swathe, in order to generate a comprehensive tomographic reconstruction of an area. The accurate differential GPS (d-GPS) positioning of the system whilst attached to the UAV allows the captured data-points to be fully geo-referenced.

Existing as a more conventional imaging tool, a standard digital camera can be also mounted under the UAV (Fig. 1c). The images obtained using this camera are saved to the device but can also be transmitted via radio-telemetry for live inspection of key facilities on a site.

## Data Processing & Visualisation

In order to process and visualise both the spatial and spectral data obtained, further software was produced at the University of Bristol (Fig. 2).

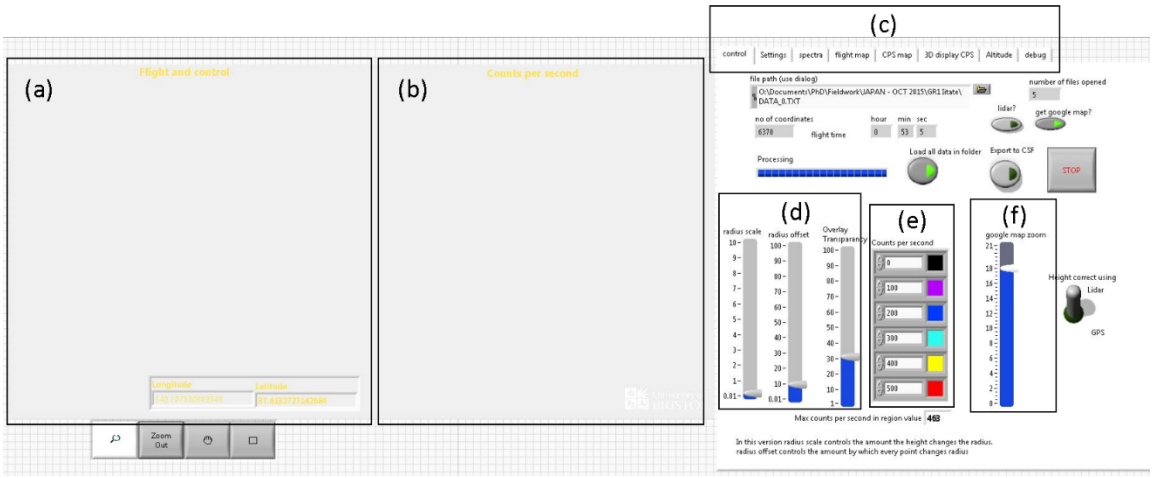


**Fig. 2.** Screenshot of the data processing software created for the project. Including; (a) plot of UAV flight paths, (b) scaled radiological intensity map overlain onto selected base-map, (c) control and calibration panels, (d) offset / radius scaling settings, (e) colouration controls and (f) map zoom level function.

Via interpolation of the GPS co-ordinates, a flight path map of the UAV over the area was constructed (Fig. 2a). Using the value for the number of incident gamma-rays received by the detector over the counting period (0.5 seconds), a scaled coloured overlay was produced by the software with the recorded value normalised for height above the ground surface as a function of the inverse square law for radiation dispersion from a point-source emitter [6,7,9]. Regions of elevated activity were represented by “hot” thermal colouration on the resulting map (Fig. 2b). These

results could then be applied to the topographic maps produced of the site via the GPS and altimeter difference subtraction discussed above (results not shown in this work).

To examine any potential differences in the isotopic signature of the contamination across the site, the software allowed for the generation of gamma-ray spectra from user-defined regions (Fig. 2b). Radiation intensity overlay maps produced of a location could be exported for manipulation and further processing within specialist graphical information and mapping software (e.g. ArcGIS™ and MatLab®), with spectral data similarly exportable for further analysis and comparison. Calibration and system setup was also undertaken within this software (Fig. 2c-f).

### Data Collection

For this work, survey flights were conducted on two separate areas of the Sellafield Ltd. nuclear site. Location 1, was a secure fenced-off compound used for the storage of multiple shipping containers holding active material, produced as a result of re-processing operations on the site. The other site, Location 2, was a large storage building, again housing material produced through the on-site processing of various active waste-streams. Both of these localities represent sites where access would typically represent a challenge (with respect to logistics and site-protocols), and dose-rate exposure to the individual performing the measurements could be substantial for measurements undertaken using traditional survey methods.

## RESULTS & DISCUSSION

### Navigational Accuracy

Prior work by the authors [7,10,11] has seen this system deployed outside of industrial settings such as this; including a disused uranium mine (Cornwall, UK) and the Fukushima-affected fallout zone. As a result, the effectiveness of the system to operate within these more constrained settings has yet to be established and is of interest with respect to safe and accurate operation on the site.

Highly-accurate mapping of contamination relies intrinsically on the highly-accurate determination of the location of the aerial platform. As such, the influence of any disturbances in the GPS position as a result of building shadowing and blind-spots are significant. To assess this, the flight paths of the UAV were studied and the degree of variance measured with respect to the pre-programmed flight paths was examined. The true flight-path maps showing the course of the system for each of the two locations (1 and 2) are shown in Fig. 3 (a and b respectively). Due to visibility constraints during the survey at Location 1 (Fig. 3a), two smaller survey flights were undertaken at differing orientations (N-S and NE-SW), in contrast to the aerial survey performed at location 2 (Fig. 3b) where the nature of the site allowed for one flight (SE-NW orientation) to be conducted over the area.

The routes programmed into the UAV for the surveys all consisted of a series of straight, equally spaced parallel lines; with the actual paths taken by the system showing good correlation to the planned routes (Fig. 3a and b). Despite both study locations existing within highly built-up areas of the site, the aerial radiation detection system is shown to exhibit only a very limited degree of flight variation. When each of the actual data points is mathematically compared to its intended location position, an average difference (deviation) of only ±0.35 m (c. 2%) is observed.

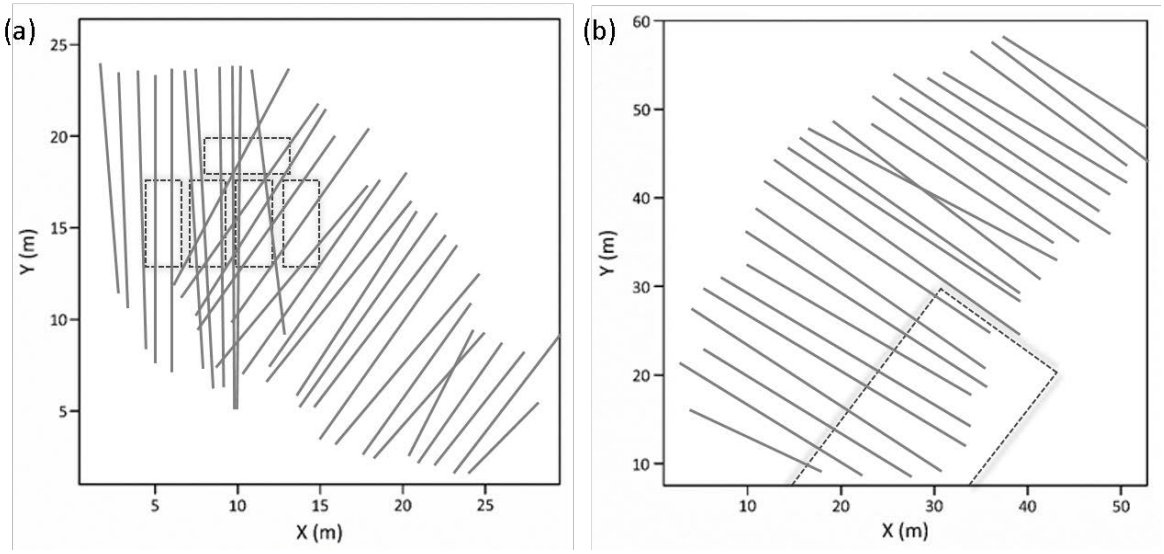


**Fig. 3.** Flight-path maps of the UAV platform for both Locations 1 and 2 (a and b respectively). The locations of the features of interest for both sites are marked.

### Location 1

The airborne radiation monitoring results for location 1 are presented in Fig. 4a. These results clearly identify the location of the five shipping-type containers located within the storage compound. Whilst the exact levels of radiation detected cannot be disclosed; this highly concentrated region of greatly elevated activity is numerous times that of the background activity of the area surrounding the compound and well-above the level recorded for the Sellafield site general background.

By selecting a user-defined area within the custom-built software, the gamma-ray spectra of the area containing this contamination was produced (not shown in this work). As was anticipated, the contributing radionuclide species include the fission product species of Sb-126, Ru-106, Eu-150, Nb-95, Zr-95, Te-133m and Eu-154 – all produced as a result of the spent-fuel separation and reprocessing that takes place on the site.

### Location 2

Similarly to location 1, the UAV radiation mapping results obtained over location 2 (Fig. 4b) – the large waste storage building, also accurately identify the position of

the radiological contamination. Apparent is the reduced level of radiation intensity detected by the aerial system (c. 80% of the peak value of location 1) during its flight over the building. However, unlike at location 1, the distribution of activity does not exactly match the outline of the structure. This difference is attributable to the stacking / storage methods that have been employed within the facility – with the higher activity material having been positioned strategically to allow its radioactivity to be attenuated by surrounding it with much lower activity wastes (a process known as "self-shielding"). As shielding of the roof of the facility does not need to exist due to the lack of traffic and people passing by, the activity level detected is observed to rise towards the centre of the structure.

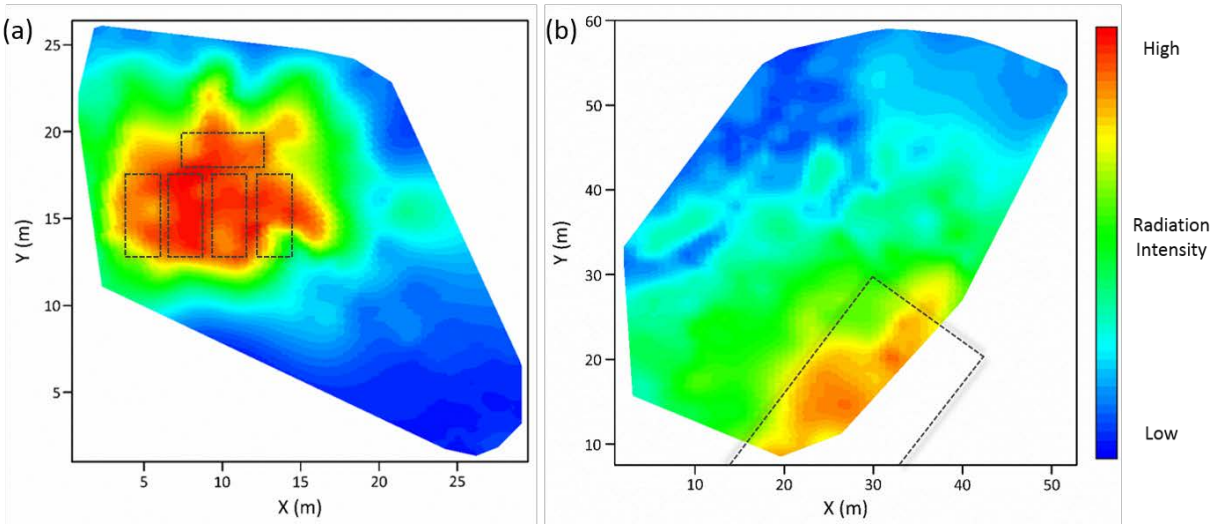


**Fig. 4.** Radiation anomaly maps produced at Location 1 (a) and Location 2 (b). A warm thermal coloured scaling identifies the location of the highest activity levels for each survey.

Again, through analysis of the gamma-ray spectra (not shown), the contributing radionuclides were identified. The species detected from this site were the medium-lived fission product Cs-137 and the activation product Co-60. Both of these species are produced in significant quantities during the nuclear fission process and are hence required to be removed as part of the reprocessing works.

## CONCLUSIONS

The aerial platform deployed within this work is demonstrated to represent a powerful tool for the assessment of radiological contamination. Following on from earlier works by the authors at other contaminated sites, the application of an unmanned aerial platform is shown to work without issue on the intricate Sellafield Ltd. nuclear site (and other such sites worldwide).

Its ability to attribute the contamination detected to specific radionuclides is an extremely powerful tool as part of an on-site remediation and monitoring programme. Whereas previously those conducting radiation monitoring around a site such as Sellafield would have been exposed to potentially significant (and possibly unknown at the time) levels of radiation, this system is able to provide results at the same high spatial resolution, with little or no dose exposure.

The versatility of the platform to undertake additional tasks whilst airborne is also of enormous advantage. Future developments of such systems with advancements in swarm behaviour and automation will further enforce the usefulness and deployability of UAVs across nuclear sites.

## REFERENCES

1. UK National Audit Office *Nuclear Decomissioning Authority - Progress on the Sellafield site: an update*; 2015.

2. US Department of Energy The Hanford Story: Overview http://www.hanford.gov/page.cfm/HanfordStory.

3. Sanderson, D. C. W.; Allyson, J. D.; Tyler, A. N.; Scott, E. M. Environmental applications of airborne gamma spectrometry. *IAEA TECDOC-827* **1995**, 71–91.

4. Beamish, D. Environmental radioactivity in the UK: the airborne geophysical view of dose rate estimates. *J. Environ. Radioact.* **2014**, *138*, 249–263.

5. Guss, P. *DOE response to the radiological release from the Fukushima Dai-ichi Nuclear Power Plant*; 2011.

6. Martin, P. G.; Payton, O. D.; Fardoulis, J. S.; Richards, D. A.; Yamashiki, Y.; Scott, T. B. Low altitude unmanned aerial vehicle for characterising remediation effectiveness following the FDNPP accident. *J. Environ. Radioact.* **2016**, *151*, 58–63.

7. Martin, P. G.; Payton, O. D.; Fardoulis, J. S.; Richards, D. A.; Scott, T. B. The use of unmanned aerial systems for the mapping of legacy uranium mines. *J. Environ. Radioact.* **2015**, *143*, 135–140.

8. AR2500 Acuity™ Acuity AR2500 Specification www.acuitylaser.com (accessed Jun 3, 2015).

9. Minty, B. R. S. Fundamental of airborne gamma-ray spectrometry. *J. Aust. Geol. Geophys.* 1997, *17*, 39–50.

10. Martin, P. G.; Payton, O. D.; Yamashiki, Y.; Richards, D. A.; Scott, T. B. High-resolution radiation mapping to investigate FDNPP derived contaminant migration. *J. Environ. Radioact.* **2016**, *164*, 26–35.

11. Martin, P. G.; Kwong, S.; Smith, N. T.; Yamashiki, Y.; Payton, O. D.; Russell-Pavier, F. S.; Fardoulis, J. S.; Richards, D. A.; Scott, T. B. 3D unmanned aerial vehicle radiation mapping for assessing contaminant distribution and mobility. *Int.*

*J. Appl. Earth Obs. Geoinf.* **2016**, *52*, 12–19.

## ACKNOWLEDGEMENTS

The authors thank Sellafield Ltd. (UK) for their support in access to areas of their site within which this study was performed. The work of the University of Bristol School of Physics Workshop is acknowledged for their assistance in the design and construction of the airframe.